DIKE NOZZLE DISPLACEMENTS

VERSION A1

DOCUMENT CONTROL				
NAMES AND SURNAMES		**POSITION**	**SIGN**	**DATE**
ISSUED BY	PRODISYS PROYECTOS CONFIABLES S.A.S.	SUBCONTRACTOR		12-07-2017
CHECKED	HERNANDO GASCA G.	MECHANICAL PROFESSIONAL		12-07-2017
APPROVED	LEONARDO TRIGOS G.	ENGINEERING LEADER		12-07-2017

ISSUES CONTROL			
VERSION	**DATE**	**ISSUE DESCRIPTION**	**REQUESTED BY**
A1	30-06-2017	INTERNAL CHECK	
C1	06-07-2017	CLIENT REVISION	

TABLE OF CONTENTS

pág.

1. SUMMARY

This report describes FEM calculations executed by Prodisys and commissioned by Seringtec SAS to study the displacements in a tank dike under various loading situations using a FEM model. The tank contains ammonia at $-33[\circ C]$ and has a dike around it to contain the ammonia in case of tank rupture. The focus of this study are the displacements of a nozzle in the dike.

In this study, this nozzle is located at $546\ [mm]$ above soil level ($N \pm 8.65\ [m]$) on the outer dike wall, see Fig. 1.1.

Figure 1.1. Nozzle location, point of interest indicated by red dot.

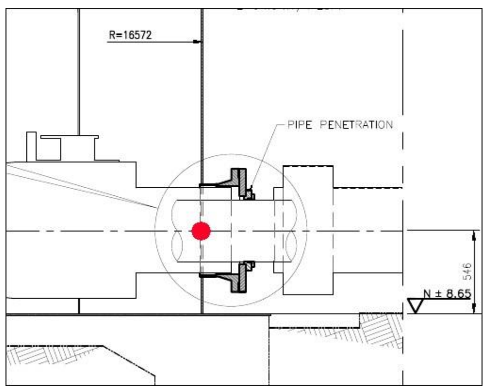

The calculated displacements of the point of interest under various independent loads are listed in the table below. Note: DY deformations include soil and foundation deformations as well.

Table 1. Displacements summary

Case	DX [mm]	DY [mm]	ANG [deg]
Case 1, Gravity	0.011	-0.010	-0.001
Case 2, weight of the roof	0.001	-0.000	-0.000
Case 3, hydro-static pressure	4.294	-0.057	-0.359
Case 4, minimum outside temperature	-1.557	-1.590	0.135
Case 5, maximum outside temperature	1.557	1.590	-0.135
Case 6, $-33[\circ C]$ of failed ammonia tank	-10.693	-6.527	0.579

Various assumptions are made in this model, and the results cannot be interpreted as exact values, but should be treated as indicative values.

2. INTRODUCTION

To this report describes FEM calculations executed by PRODISYS and commissioned by SERINGTEC SAS to study the displacements in a tank dike under various loading situations.

Figure 2.1. Cross section of the tanks with the dikes (blue) around them.

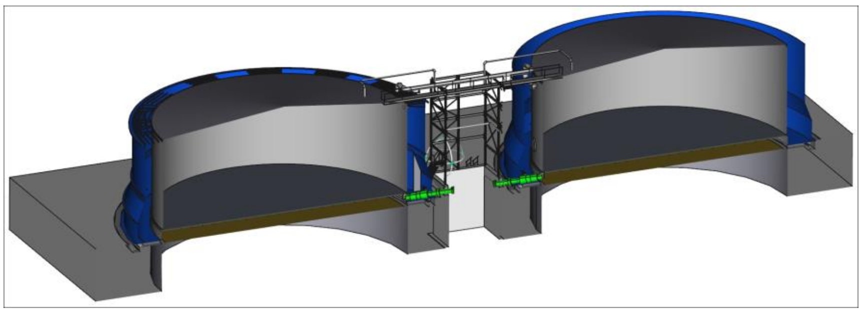

The tank contains ammonia at −33[∘C] and has a dike around it to contain the ammonia in case of tank rupture. This study calculates the displacements of a nozzle in the dike using a FEM model. The nozzle (near green) is located at 546 [mm] above soil level (N ± 8.65 [m]) on the outer dike wall, see Fig. 2.2.

Figure 2.2. Nozzle location indicated by red dot: point of interest (POI).

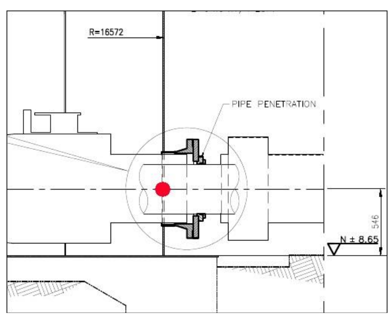

2.1. OBJECTIVE

To objective of this study is to provide indicative displacements of the tank nozzle for in the following independent cases:

1. Gravity
2. Roof load
3. Hydro-static pressure of Ammonia
4. Intact interior tank, dike exposed to minimum outside temperature: 20[∘C]
5. Intact interior tank, maximum outside temperature: 40[∘C]

6. Failed interior tank, ammonia of $-33[°C]$ on the inside of the dike exposed to average outside temperature: $30[°C]$ in the soil for case 4, 5 and 6, the reference temperature is set at average outside temperature of: $30[°C]$.

2.1 METHOD

An axi-symmetric FEM model is made of the tank, including the foundation. In reality, the tank is not completely axi-symmetric. Near the nozzle, a piece of the inner wall is missing. Therefore, the inner-wall is not modeled at all, which is conservative (giving larger displacements). In *APPENDIX E - Impact including inner wall in model on results*, the inner-wall is included in the model to evaluate its (minor) impact on the results. Gravity is applied as body loads and Thermal loading as temperatures at the model boundaries. It's assumed that quasi-static linear theory is sufficient to obtain the nozzle displacements, hence the different results can be superimposed onto one another. The results are displayed in tabular form in this report.

2.2 SCOPE

Scope of this study is to provide indicative values or value ranges for the nozzle displacements under various external quasi-static conditions. Various simplifications and assumptions in the model do not allow an exact or transient prediction of these displacements. It is recommended to verify the presented predictions using measurements or more advanced simulations. Deformations due to wind load are outside this study scope.

2.3 OUTLINE

The FEM model and solving the model is described in chapter 3. Chapter 4 presents the FEM results. Chapter 5 presents conclusions and recommendations.

3. FEM MODEL

This model describes the FEM model used for the dike simulations.

3.1 THE FEM MODEL

This paragraph describes the FEM model. The FEM model is based on the following data sources:

- drawing: NAM-MEM-003_12, rev 0, Ingeneria de detaille diques tanques 30A / 30B amoniaco dessarollo de láminas dique TK30A/30B, for the dike sheet geometry

- drawing: NAM-MEM-003_11, rev 0, AB-2105-003, Ingenieria de detaille diques tanques 30A/30B amoniaco detailles generales, for the details of the fixation
- CAD Step file: 'Ensamble_General.stp', last modified 16 June 2017, 14:04:09 CEST, for the geometry of the ring stiffeners and foundation.
- report: Memoria de Calculo Mecanico Dique, NAM-MEC-001, version 0, NAM-MEC-001-0_Calculo_mecanico_dique.pdf, for the material properties.

See Appendix A for an image of the drawings.

Various values used in the model are not available in the above data sources. These values are assumed, based on common technical literature. By no means these assumptions are accurate to represent the real situation. Therefore, the presented results in this report are only indicative. Appendices *APPENDIX C Impact of soil size and properties on results* (page 31) and *APPENDIX D - Impact of mesh size on results* (page 33) study the impact of some of those assumptions, but this is by no means sufficient to call it an accurate deformation prediction.

3.1.1 Software

The FEM model is created and results are extracted using Salomo-Meca V2016.0 LPGL[1]. The model is solved using Code_Aster, version 12.6[2], both open source code for structural and thermo-mechanical analysis, maintained by EDF, France[4].

3.1.2. Units

The FEM model is made using S.I. units. Temperatures are expressed in degrees Celcius, as Temperatures are only considered as relative values, not in any absolute sense.

This report presents values with its units.

3.1.3. Coordinate system

The origin of the coordinate system is located in the center of the tank at level $N = 8.65\ [m]$ which is more or less the soil surface level.

- the X-axis points towards the other tank, pointing right,

[1] https://en.wikipedia.org/wiki/Finite_element_method
[2] http://code-aster.org/UPLOAD/DOC/Presentation/Plaquette_SALOME_V7.pdf
[3] http://code-aster.org/UPLOAD/DOC/Presentation/plaquette_aster_en.pdf [4] https://www.edf.fr/groupe-edf/espaces-dedies/edf-les-start-up

- the Y-axis is the central axis at, pointing up,
- the Z-axis is pointing out of plane, orthogonal to X and Y-axis.

3.1.4. Geometry

The axi-symmetric FEM model is build using the solid modeling facility; first vertices, lines and areas are defined. The areas are grouped into one compound that can be transferred to the meshing facility. Within the compound, several area, line and vertex groups are defined for later processing in the meshing facility.

The geometry model contains the shape of 3 different material objects:

- The dike in ASTM A-516 Grade 60 steel.
- The foundation in concrete.
- A part of the soil supporting these structures, with the sizes $R_{o,soil} = 2 \cdot R_{o,dike,bottom}$ and $H_{soil} = 10\ [m]$. In *APPENDIX C - Impact of soil size and properties on results* (page 31) the impact of the assumed soil size on the overall results is calculated.

The tank is not completely axi-symmetric. Near the nozzle, a piece of the inner wall is missing. Therefore, the inner-wall is not modeled at all, which is conservative (giving larger displacements). In *APPENDIX E - Impact including inner wall in model on results* (page 34), the inner-wall is included in the model to evaluate its (minor) impact on the results.

The maximum liquid volume of the ammonia is $6042\ [m^3]$. When the liquid is contained by the dike, the level of the ammonia fluid is estimated to be at $8.433\ [m]$ above the foundation.

Some details are simplified in the model:

- The soil is assumed to be flat, while in reality it also holds the inner tank and it's foundation. Not modeling the inner tank and foundation changes the local temperature distribution in the soil near the tank. Here is assumed that this does not change the deformation at the point of interest.
- Only a part of the soil is modeled. Only a static temperature distribution is calculated, with an average far away temperature of 30[∘C] at the edges where the soil is cut off from the rest of the world. Therefore, the size and shape of the modeled soil determines the temperature distribution and hence, the deformations of the nozzle. The impact of the size and shape of the modeled soil is studied in APPENDIX C - Impact of soil size and properties on results (page 31). Alternatively, a transient thermal analysis can be made where the evaporation of the ammonia is simulated. In such an analysis, the soil will cool down and after the complete evaporation heat up again. The deformation of the nozzle can be estimated as a function of time. However, transient analysis falls outside the scope of this study. See also: Paragraph Solving (page 13).

Figure 3.1. Nozzle location indicated by red dot: point of interest (POI).

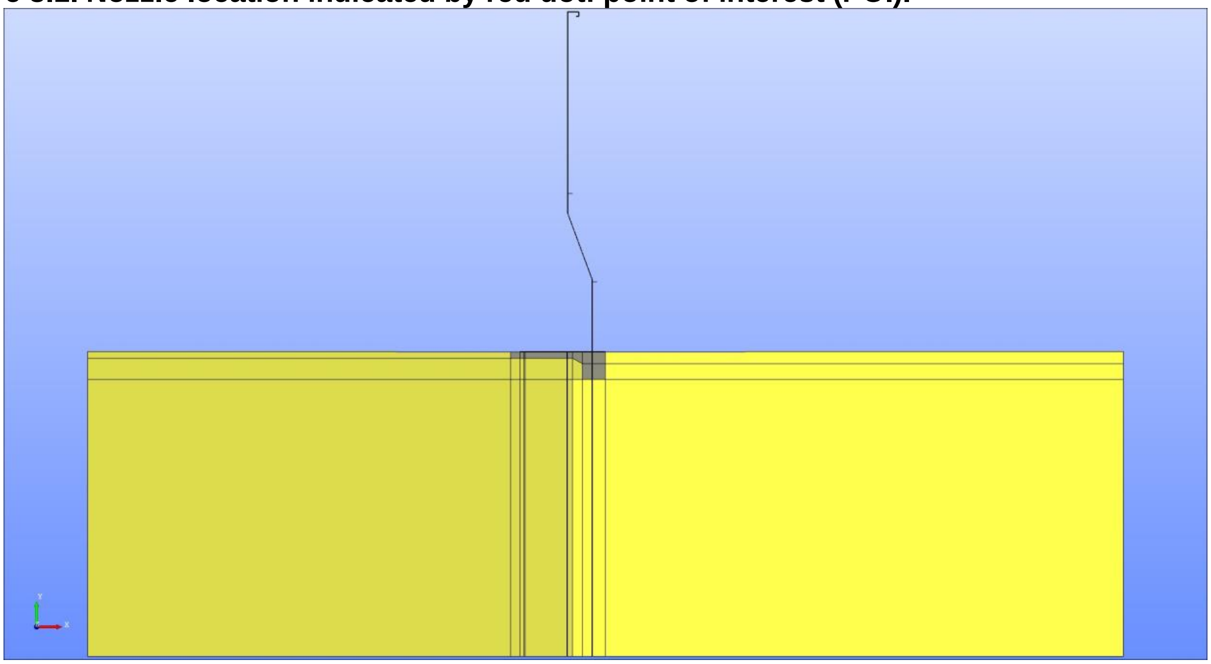

- The (Hilti) bolts used to fix the tank to the foundation are not modeled. The bottom plate is simply connected to the foundation. As both steel and concrete have the same thermal expansion coefficient and transient effects are ignored in this study (see paragraph Solving (page 13)).

- Transitions between conical sheets and vertical sheets are straightened at the corners, see Fig. 3.3. The effect on the overall dike stiffness is negligible.

3.2 ELEMENT MESH

The solid geometry is divided into nodes and elements using the mesh generator of the Salome-Meca program. Here, a mapped mesh is applied.

As deformations are studied, not derivatives such as strains or stresses, the mesh can be relatively coarse for still accurate results. Still, 4 elements are used over the cross-section and all other areas have 15 divisions. In *APPENDIX D - Impact of mesh size on results*, the impact of mesh size on the results is studied. The FEM model contains 27101 nodes and 10734 elements.

3.1.1. Element types

The element used in the model is a 2D axi-symmetric QUAD8 element with four corners and four midside nodes. In the thermal analysis, the degree of freedom at each node is TEMP and in a mechanical analysis: DX, DY. This element is used for all solid geometry.

1D SEG3 elements are used to define the surface loads on the edges of the QUAD8 elements.

The model contains 2012 SEG3 and 8722 QUAD8 elements.

Figure 3.2. Zoom in on the dike part of the model.

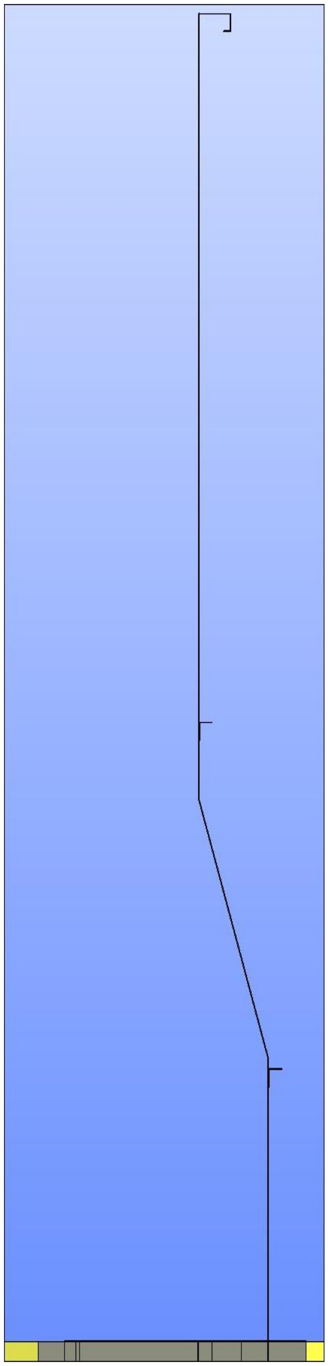

Figure 3.3. Zoom in on the simplifications of the conical section transitions.

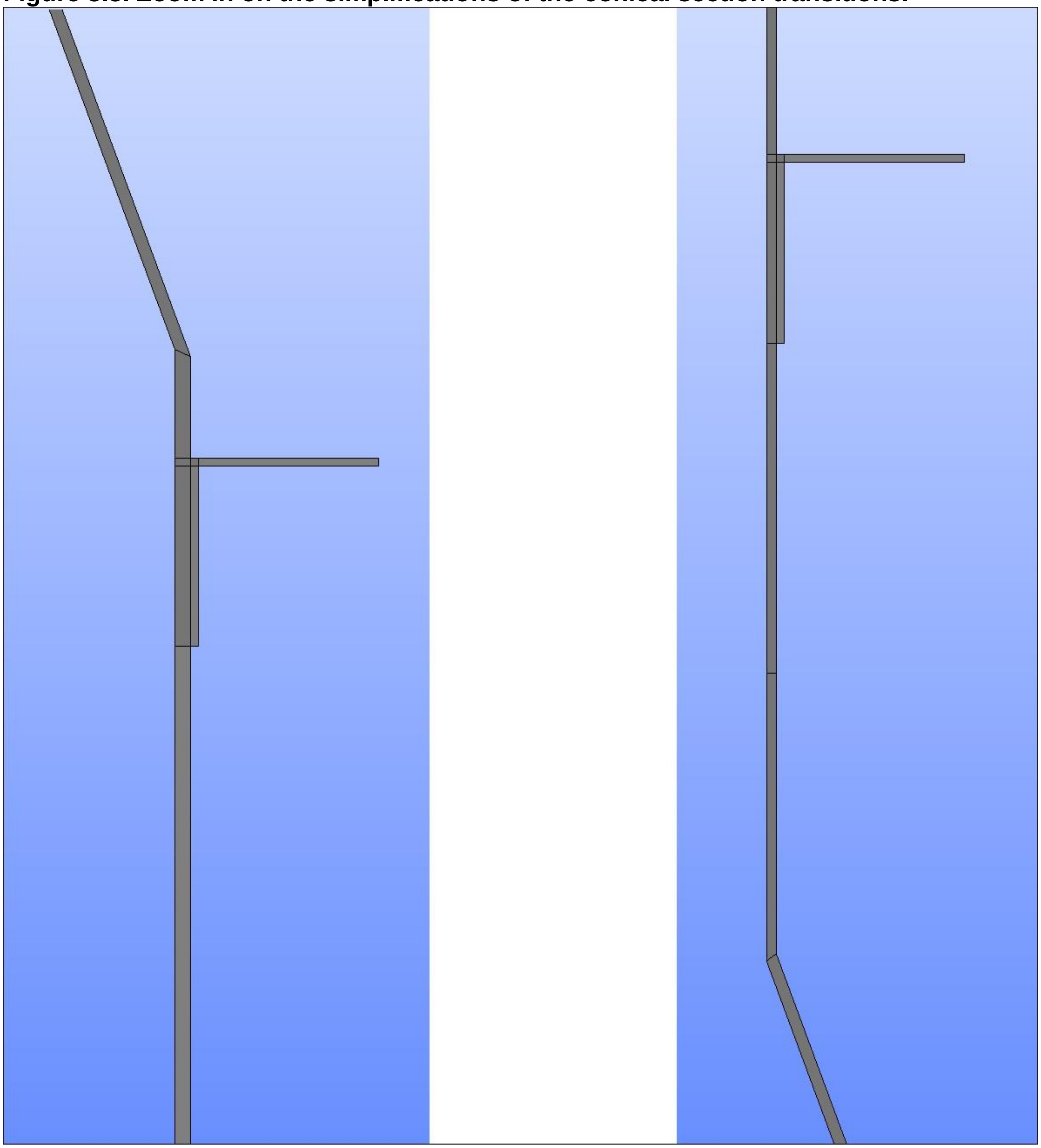

Figure 3.4. Overview of the element mesh.

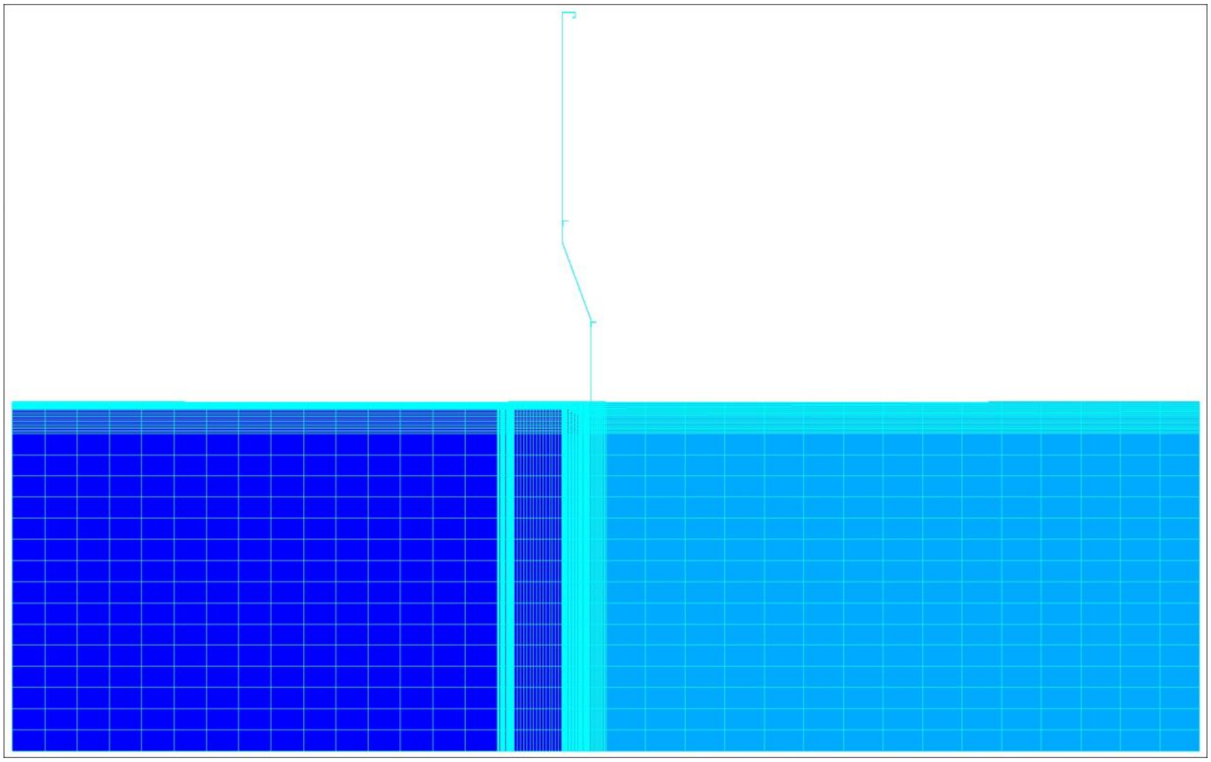

Figure 3.5. Element mesh, zoom in on detail around the bottom plate.

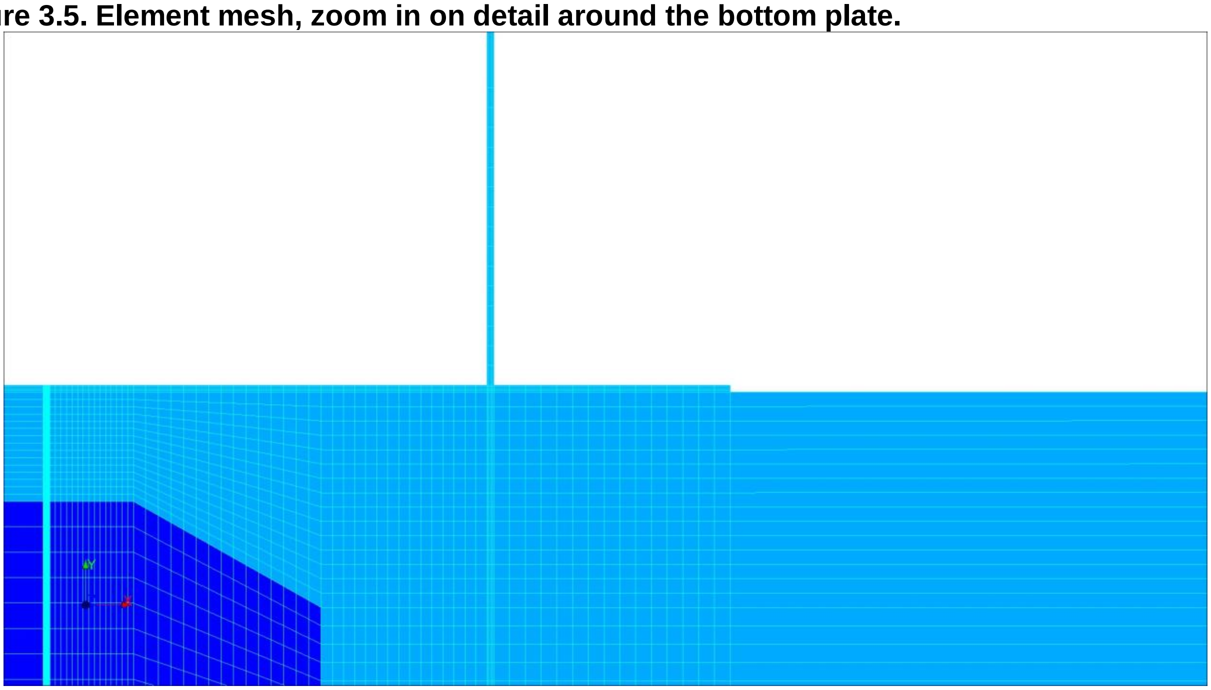

Figure 3.6. Element mesh, zoom in on lower stiffener.

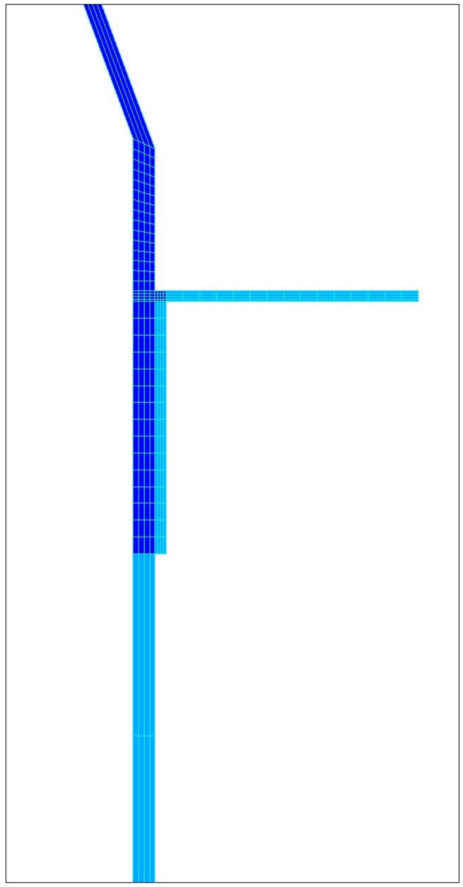

Figure 3.7. Element mesh, zoom in on upper stiffener.

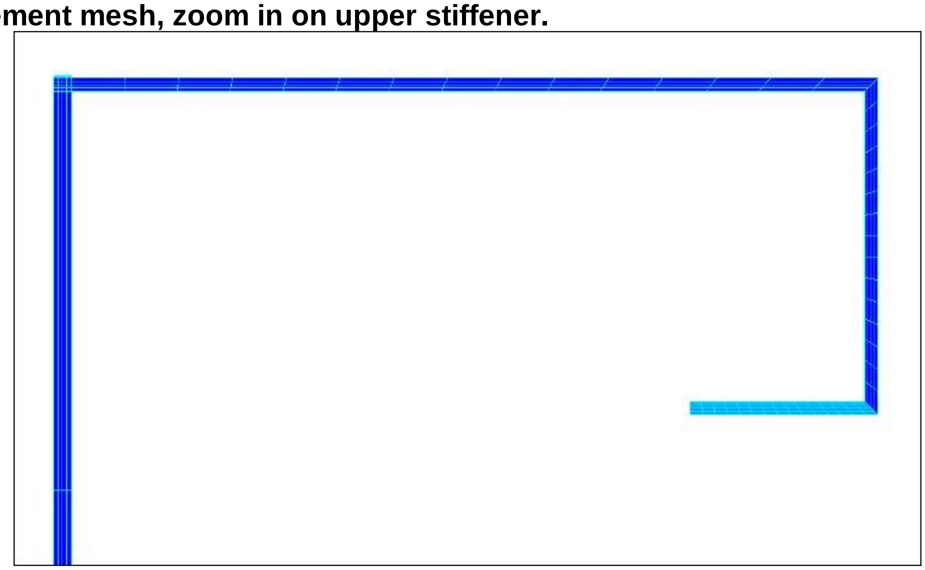

3.1.2. Material

The dike is made of ASTM A-516 Grade 60 with impact test at $-50[°C]$. The foundation is made of Concrete. The concrete and soil properties are unknown. Values for the concrete and the soil are assumed based on averages in generic technical literature. The material properties used in the FEM calculation are given in the table below:

Table 3.1: Material properties

Material	Density ρ $[kg/m]$	Elasticity $E[Pa]$	Poisson ratio ν $[-]$	Thermal expansion coefficient α $[m/mK]$	Thermal conductivity coefficient λ $[W/mK]$
ASTM A-516 Grade 60	7800	$210 \cdot 10^9$	0.3	$12 \cdot 10^{-6}$	80
Concrete	2300	$28 \cdot 10^9$	0.2	$12 \cdot 10^{-6}$	$10 \cdot 10^{-6}$
Soil	1300	$24 \cdot 10^6$	0.45	$12 \cdot 10^{-6}$	$2 \cdot 10^{-6}$
Ammonia at $-33[°C]$	700	$-$	$-$	$-$	$-$

In *APPENDIX C - Impact of soil size and properties on results* the impact of the assumed soil properties on the overall results is calculated.

3.3 BOUNDARY CONDITIONS AND LOADS

The figure below shows the definitions of the boundaries in the model. The boundary conditions are applied here. The different independent load cases applied to the model are listed below. As quasi-static linear theory is applied, the below cases can be combined using (scaled) superposition to study combined loading situations.

3.3.1. Case 1: Gravity

Gravity is applied as a body load of −9.81 [m/s2].

3.3.2. Case 2: Roof Load

Plates weight of corroded roof is $54935.5\ [N]$. The weight is a applied as a pressure on the dike top (thickness $7.9375\ [mm]$) of: $p = 69888\ [Pa]$.

3.3.3. Case 3: Hydro-static pressure of Ammonia

The hydro-static pressure of the ammonia in case of inner tank rupture is modeled as pressure, perpendicular to surface of the ammonia-dike interface, see Fig. 3.9.

The value of the pressure is a function of the height $y`abovethelowestammonialevelandisapplieduntil$: $math$: ‘$y = H = 8.433\ [m]$ above the lowest ammonia level. The pressure level as a function of height $p(y)$ is defined as: $p(y) = \rho_{ammonia} \cdot g \cdot (H - y)$

3.3.4. Case 4: minimum outside temperature

This load case considers an intact interior tank, with the dike exposed to minimum outside temperature of: $20[^{\circ}C]$.

The thermal load is defined as (see Fig. 3.9):

- All outside boundaries, except soil bottom and side interface are set to $20[^{\circ}C]$.
- The soil bottom and side interface are set to $30[^{\circ}C]$, the average temperature between maximum and minimum temperature.

As the tank is intact, in reality, the area under the tank is probably colder than calculated here due to the $-33[^{\circ}C]$ ammonia in the tank. It is assumed that this effect is negligible, especially for studying the difference between minimum and maximum temperature, the next load case.

For the calculation of deformations, a reference temperature of $30[^{\circ}C]$ is used, the average outside temperature.

Figure 3.8. Surface where outer temperature is applied, lower stiffener zoom in.

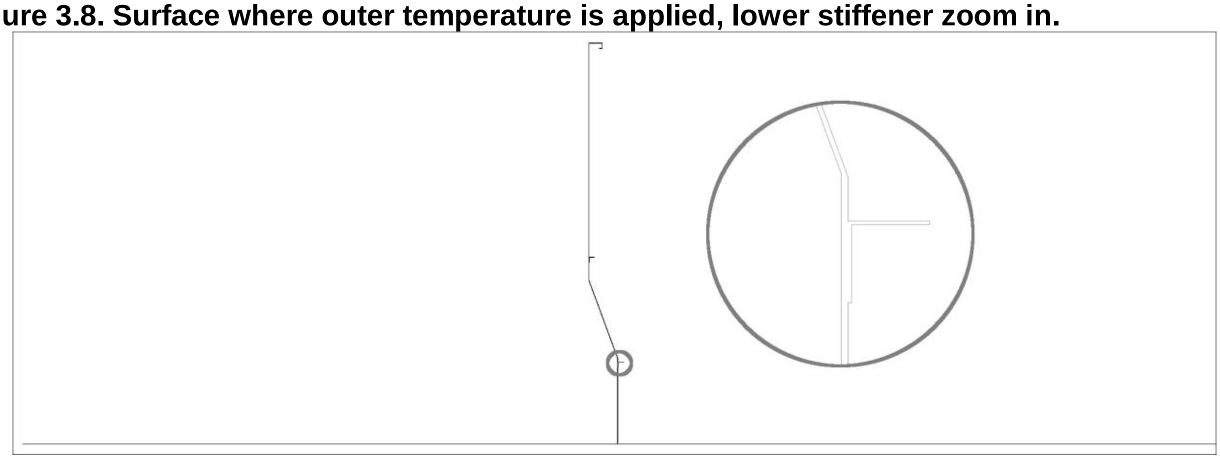

To determine the thermal deformation, 2 calculations are made in sequence. First a thermal distribution is calculated, followed by a mechanical analysis that calculates the deformation as a consequence of the thermal distribution.

To calculate the thermal deformation, the following mechanical boundary conditions are applied.

- The thermal distribution as calculated as above.
- Displacements in vertical direction (DY) constrained at the soil bottom interface.
- Displacements in radial direction (DX) constrained at the soil side interface.

3.3.5. Case 5: Maximum outside temperature

Case 5 is equal to case 4 only now, all the outer surfaces are exposed to maximum outside temperature of: $40[°C]$.

3.3.6. Case 6: Thermal deformation due to failed inner tank

This case considers a . failed interior tank, ammonia of $-33[°C]$ on the inside of the dike exposed to average temperature in the soil of: $30[°C]$.

The thermal load is defined as (see Fig. 3.9):

- The ammonia interface is set to $-33[°C]$.
- The soil bottom and side interface are set to $+30[°C]$, the assumed average temperature at the site.

To calculate the thermal deformation, the following mechanical boundary conditions are applied.

- The thermal distribution as calculated as above.
- Displacements in vertical direction (DY) constrained at the soil bottom interface.
- Displacements in radial direction (DX) constrained at the soil side interface.

Figure 3.9. Location of boundary conditions and loads in Case 6.

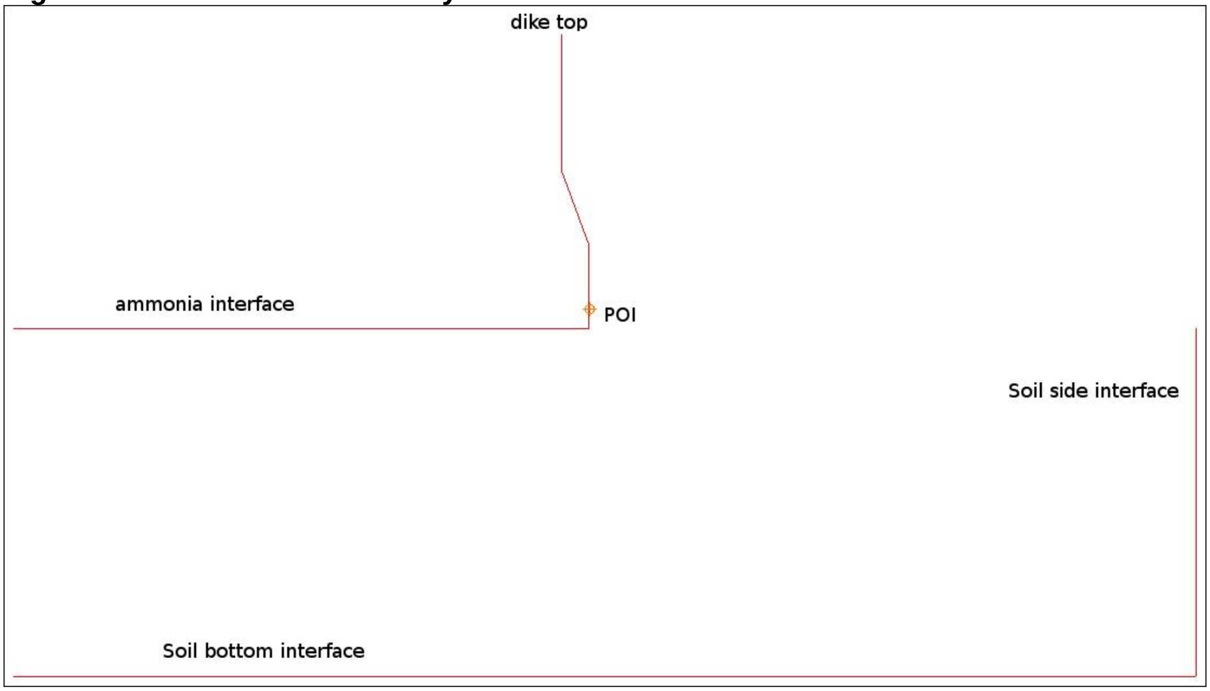

3.4 SOLVING

Only a quasi-static analysis is made, no transient effects or contact effects are studied.

The FEM model is solved on a four core-i5 platform running linux mint 18.1 with 8 GB of ram memory. The geometry and mesh are generated in a few seconds. Solving the model, all load cases takes about 30 seconds.

4. FEM RESULTS

This chapter presents the FEM results. When deformed shape is shown, generally a scale factor of 50 is used on the deformations. The shape of the deformed shape is defined by all deformation components, DX and DY. The color of the deformations can be either "Magnitude", "DX" or "DY", as indicated in the legend of the plots.

First a global presentation of all load cases is given. Specific results such as deformations of the point of interest and the reaction forces are discussed in subsequent paragraphs.

4.1. FULL MODEL RESULTS

This paragraph presents FEM result images.

Figure 4.1. Case 1: Gravity, deformation in radial direction, zoom in on POI.

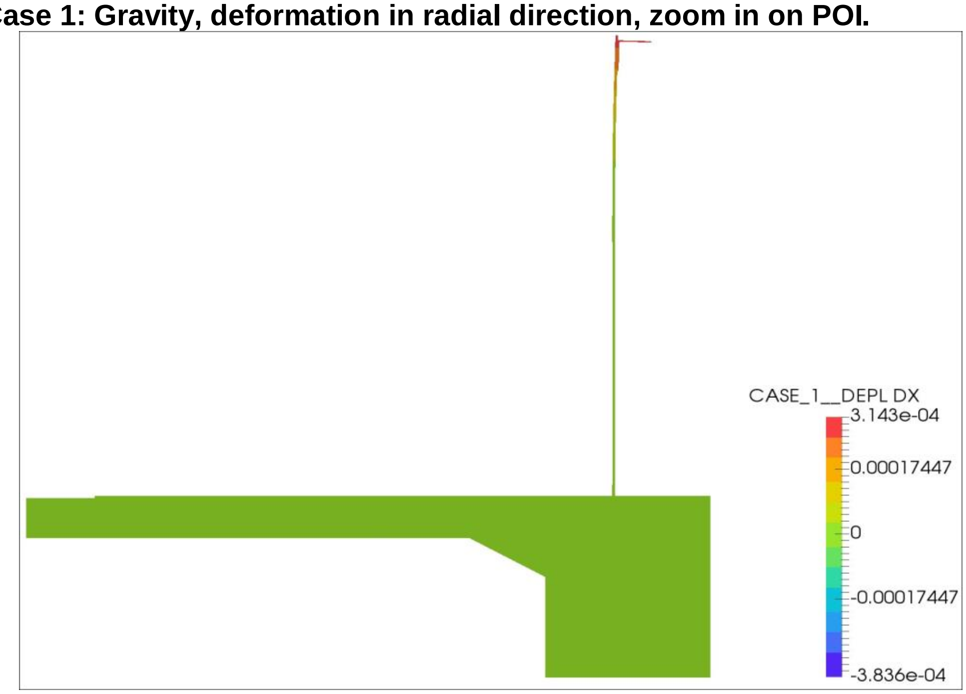

Figure 4.2. Case 2: Roof load, deformation in radial direction, zoom in on POI.

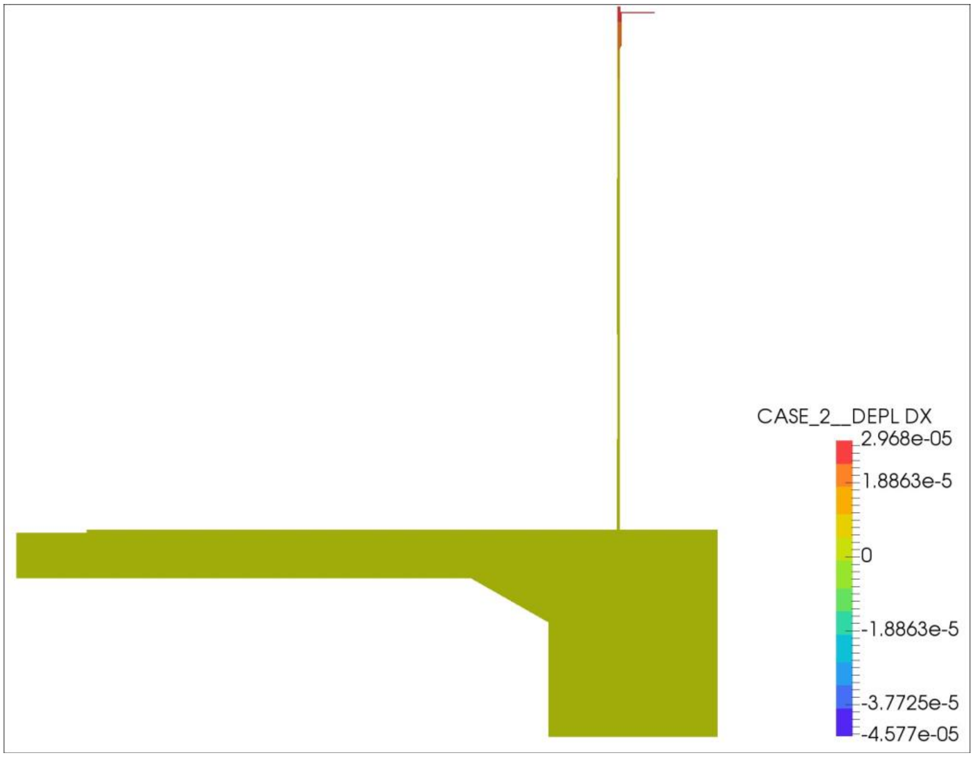

Figure 4.3. Case 3: Hydro-static pressure of Ammonia, deformation in radial direction, zoom in on POI.

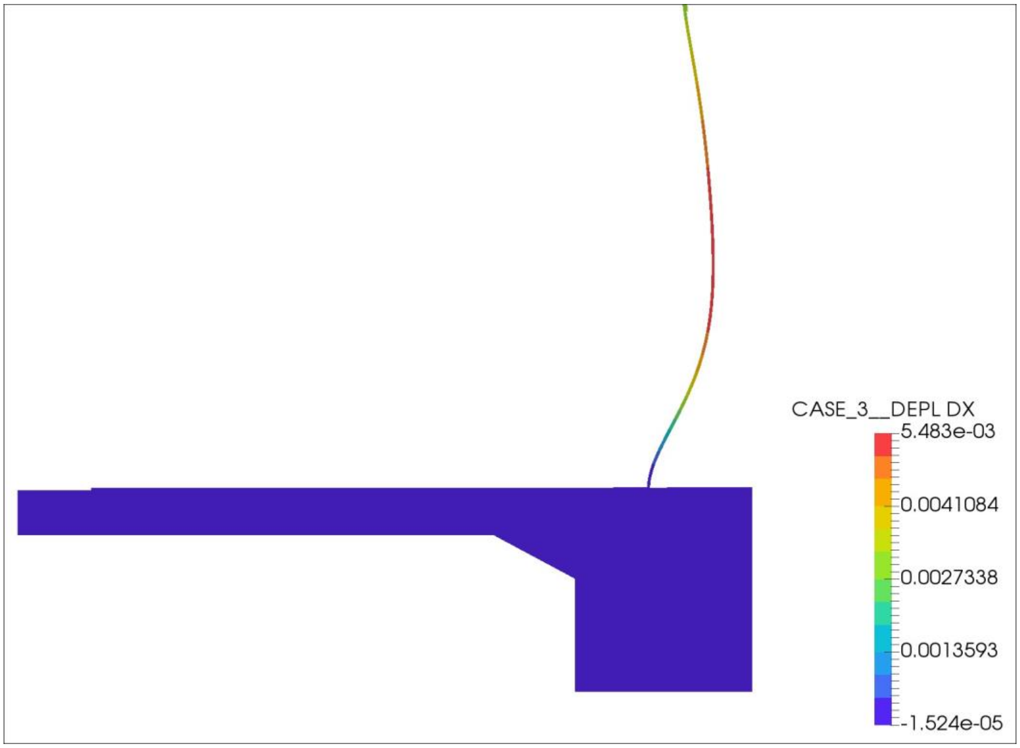

Figure 4.4. Case 4: minimum outside temperature, Temperature distribution.

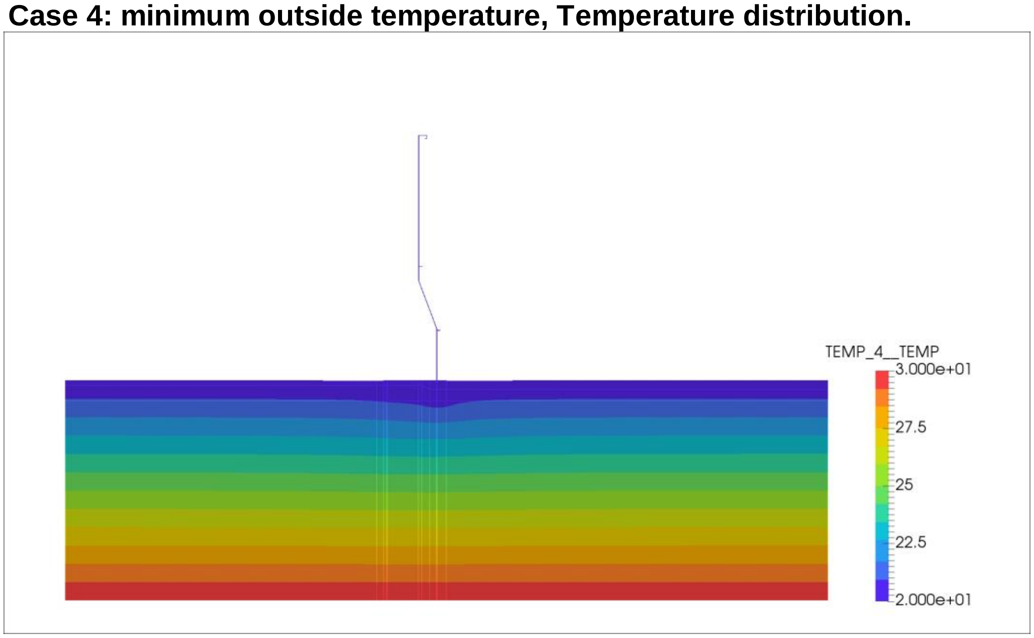

Figure 4.5. Case 4: minimum outside temperature, deformation in radial direction, zoom in on POI.

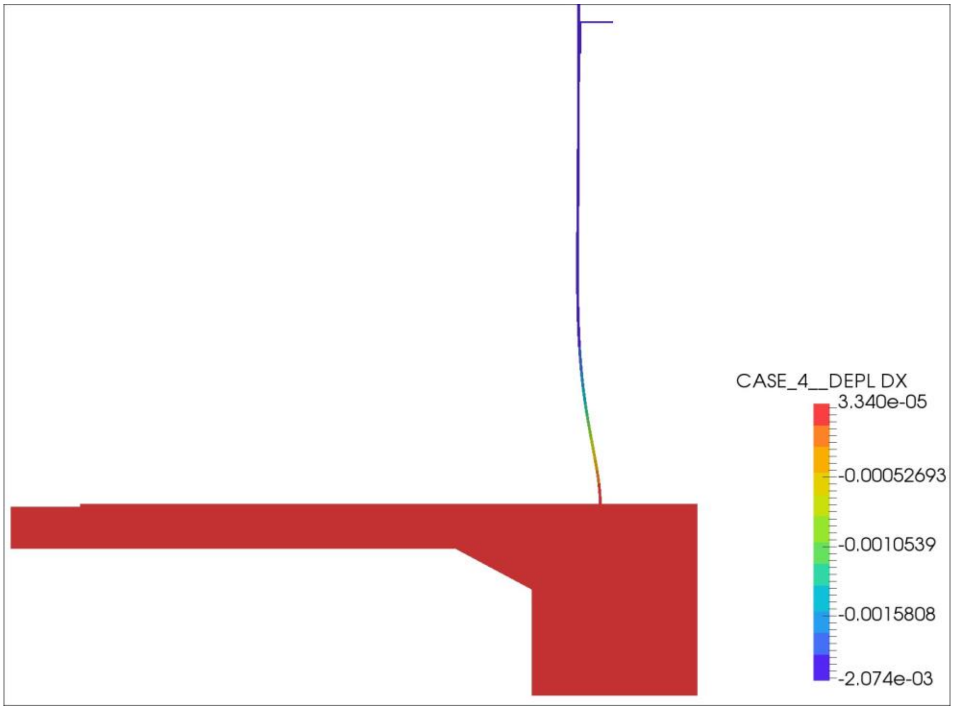

Figure 4.6: Case 5: maximum outside temperature, Temperature distribution.

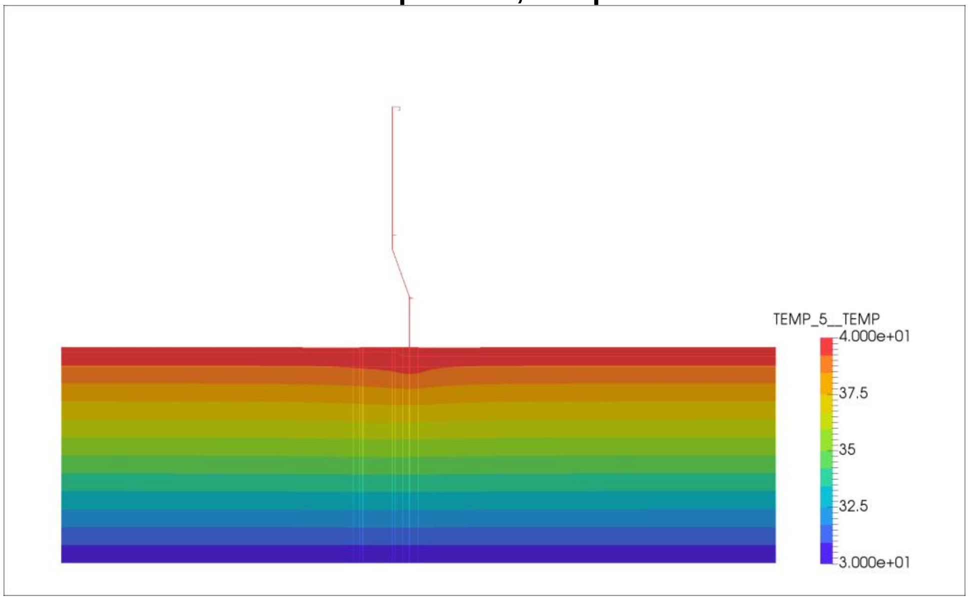

Figure 4.7: Case 5: maximum outside temperature, deformation in radial direction, zoom in on POI.

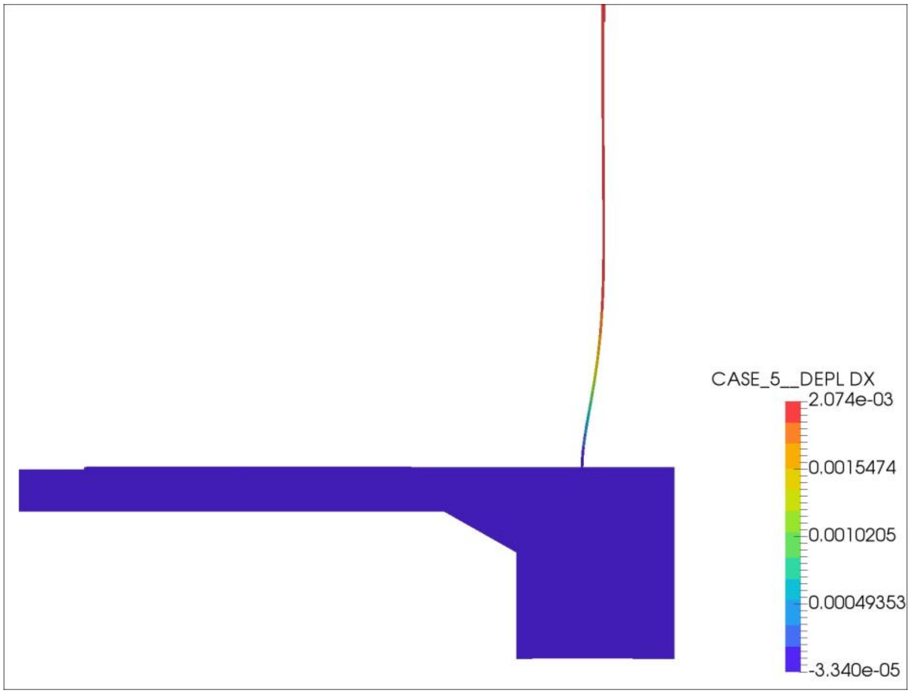

Figure 4.8: Case 6: Thermal deformation due to failed inner tank, Temperature distribution.

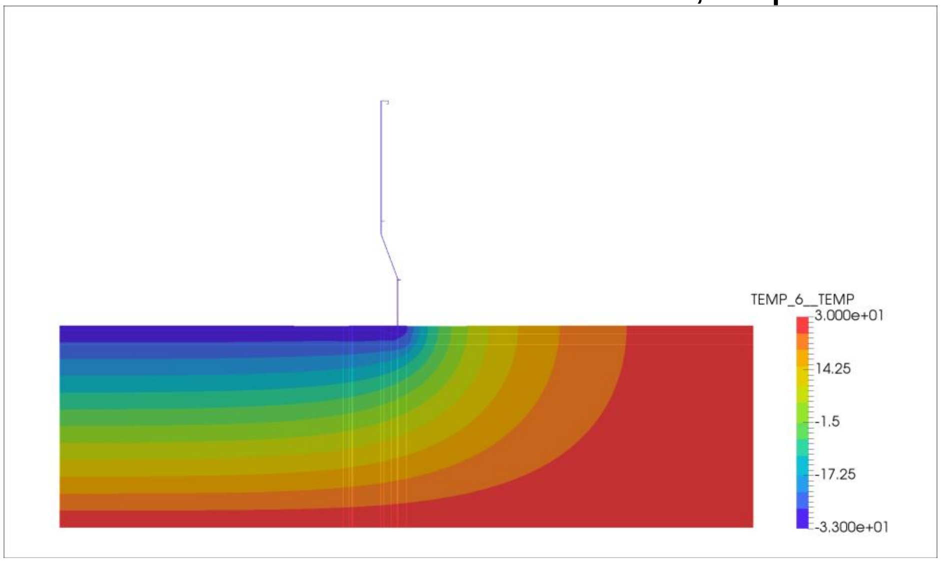

Figure 4.9: Case 6: Thermal deformation due to failed inner tank, deformation in radial direction.

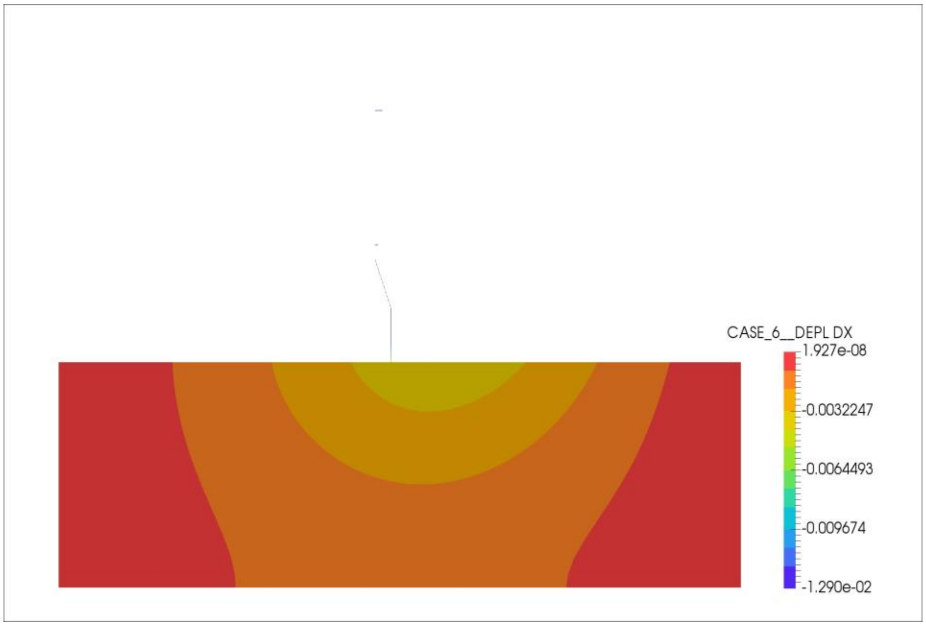

Figure 4.10: Case 6: Thermal deformation due to failed inner tank, deformation in radial direction, zoom in on POI.

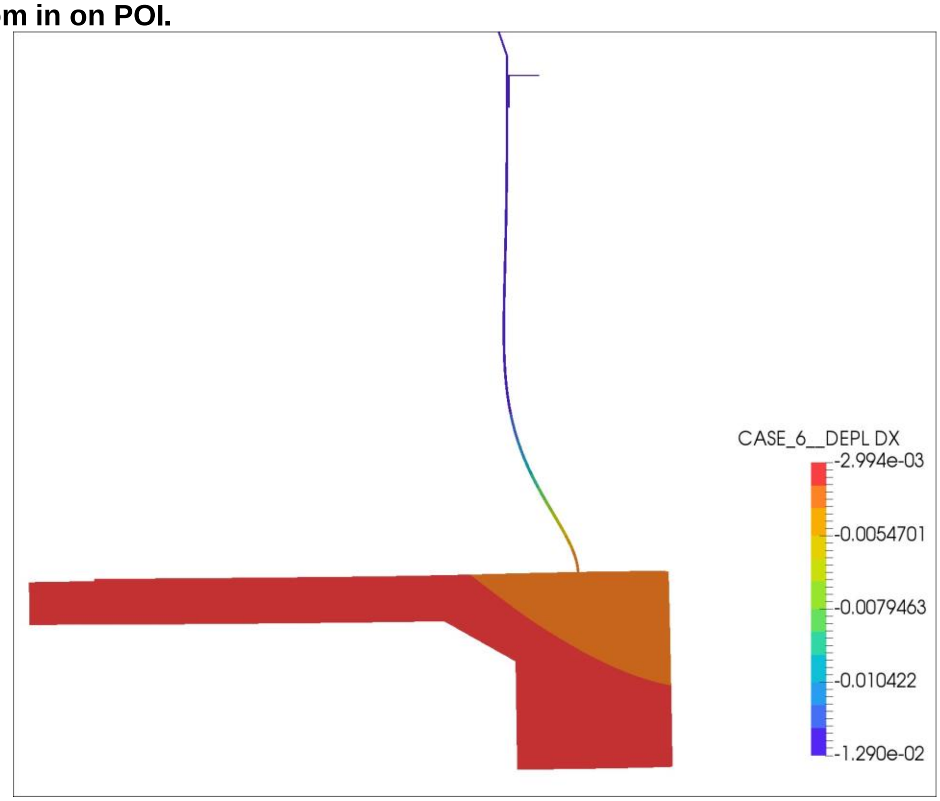

Figure 4.11: Case 6: Thermal deformation due to failed inner tank, deformation in vertical direction.

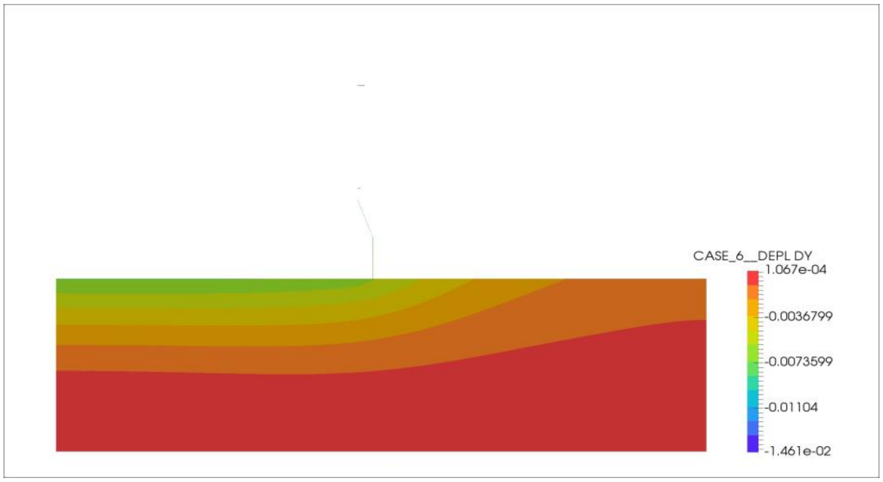

4.2. POI DEFORMATIONS

The deformations of the nozzle (poi) are given in the table below. The location of the POI is defined in the Introduction. A positive angle ANG is defined from x-axis towards the y-axis, as usually in Cartesian coordinate systems. The angle ANG is calculated by considering a point on the inside of the dike wall, exactly opposite of our point of interest.

Case	DX [mm]	DY [mm]	ANG [deg]
Case 1, Gravity	0.011	-0.010	-0.001
Case 2, weight of the roof	0.001	-0.000	-0.000
Case 3, hydro-static pressure	4.294	-0.057	-0.359
Case 4, minimum outside temperature	-1.557	-1.590	0.135
Case 5, maximum outside temperature	1.557	1.590	-0.135
Case 6, $-33[{}^\circ C]$ of failed ammonia tank	-10.693	-6.527	0.579

Note:

1. DY deformations include soil and foundation deformations as well.
2. Case 4 and 5 have opposite results, as expected.
3. A manual calculation of Case 3, taking a assuming an unconstrained steel dike with a mean radius of $R_{dike} \approx 16.565\ [m]$, a thickness of $t_{dike} = 0.0127\ [m]$ exposed to an internal pressure of $p(0.546) = \rho_{ammonia} \cdot g \cdot (8.433 - 0.546) = 54160\ [Pa]$. The nominal stress in tangential direction is approximately: $\sigma_t \approx \frac{p \cdot R_{dike}}{t} \approx 70.6\ [MPa]$, with an elongation in circumferential direction of:

$\Delta L = \frac{\sigma_t \cdot 2 \cdot \pi \cdot R_{dike}}{E} = 0.035[m]$ which corresponds to a radial expansion of (dividing by 2π) $DX_{analytic} = 5.57\ [mm]$. The ratio between FEM and analytic is almost 30%. The soil that prevents the dike to expand radially is not exposed to radial pressure itself. Therefore, the difference is relatively large.

4. A manual calculation of Case 6, assuming an unconstrained steel dike with a radius of $R_{dike} = 16.572\ [m]$, exposed to a temperature difference of $\Delta T = -63[°C]$ relative to average temperature of $30[°C]$ will expand $-12.5\ [mm]$ (contract). This is fairly close to the DX results in the table. The difference can be explained by the inclusion of soil and foundation in the FEM calculations. The ratio between FEM and analytic is almost 17%. The difference is smaller than in case 3 and can be explained by the fact that the soil is now also exposed to the same loading as the dike: the low temperature. Hence the soil also contracts radially, thereby giving less resistance to the dike contraction.
5. In *APPENDIX E - Impact including inner wall in model on results* (page 34), the inner-wall is included in the model to evaluate its impact on the results. For case 6, the largest impact is observed: $0.03\ [mm]$ less DX deformation. The change for cases 4, 5 and 6 is approximately 0.3%. The results are similar for all cases, except for case 1: gravity. The full method and results can be found in the appendix.

$$\Delta R = \alpha_{steel} \cdot R_{dike} \cdot \Delta T = -0.0125\ [m]$$

An additional reference point is defined at the same radius as POI, vertically at the interface between dike bottom plate and foundation. This point is referred to as 'Pbot'. The relative displacements between POI and Pbot are defined as:

$$DDX_{POI} = DX_{POI} - DX_{Pbot}$$

$$DDY_{POI} = DY_{POI} - DY_{Pbot}$$

The calculated relative displacements DDX and DDY are listed below:

Case	DDX [mm]	DDY [mm]
Case 1, Gravity	0.011	-0.002
Case 2, weight of the roof	0.001	-0.000
Case 3, hydro-static pressure	4.289	-0.053
Case 4, minimum outside temperature	-1.544	-0.067
Case 5, maximum outside temperature	1.544	0.067
Case 6, $-33[°C]$ of failed ammonia tank	-6.711	-0.423

Note:

1. The vertical relative displacement in case 6 is now almost equal to a manual calculation:

ΔL = Hpoi · αsteel · ΔT = 0.546 · 12 · 10−6 · −63 = −0.4128:

4.3. REACTION FORCES

The table below gives the reaction forces in vertical direction. As the model is axi-symmetric, reaction forces are given per radians. One must multiply the model results with a factor 2π in order to obtain the real reaction forces.

Case	FY model [N]	FY reality [N]
Case 1, Reaction forces divided by 2 pi Case 1, Gravity	74072130	4.654e+08
Case 2, Reaction forces divided by 2 pi Case 2, weight of the roof	8743.256	54935.498
Case 3, hydro-static pressure	7501865	47135607.944

Note:

1. The reaction forces also include weight of soil and foundation.
2. The roof weight corresponds well with applied load 54935.5 [N]
3. The ammonia volume is recalculated from the reaction forces with the equation:

This volume is much more than stated in Geometry. The difference can be explained by the inner tank absence in the FEM model. The impact on the displacements of the POI is probably negligible, because that is mostly driven by local deformations of the dike shell, as can be seen in Fig. 4.3.

5. CONCLUSIONS AND RECOMMENDATIONS

5.1. CONCLUSIONS

The FEM calculations present up to 30% reduction in the radial deformations of the nozzle (our point of interest) compared to analytic equations. The differences can be explained by the connection of the dike to foundation and soil. Also vertical and angular deformations are presented.

Several uncertainties in the FEM modeling approach are tested and can change the results to a minor extend. The next paragraph presents recommendations for more accurate deformation predictions.

5.2. RECONMENDATIONS

The following recommendations are made to refine the results of this study and to increase its validity:

- include the inner tank foundation in the FEM model.
- update the material properties for concrete and soil with more realistic values used at the considered structure.
- consider making transient analysis to get more realistic temperature distributions.
- validate minimum and maximum temperature deformations, Case 4 and 5, using measurements.
- validate if there exist any kind of thermal isolation between ground and Dike in that reduces the DY soil displacements.

6. APPENDIX A – FILES

Root directory: /Projects/2017/2017-06-26-Seringtec-dike received information:

./Corresp/2017-06-26-01-initial-info:

- Ensamble Corte 1.pdf
- Ensamble Corte 2.pdf
- Ensamble Corte 3.pdf
- Ensamble Corte 4.pdf
- Ensamble Corte 5.pdf
- NAM-ICG-005_Análisis de dispersión fuga amoniaco_Rev 0.pdf

./Corresp/2017-06-26-01-initial-info/Info Dique:

- NAM-ICG-005_Análisis_de_dispersión_fuga_amoniaco_Rev_0.pdf
- NAM-MEC-001-0_Calculo_mecanico_dique_Anexo1.pdf
- NAM-MEC-001-0_Calculo_mecanico_dique_Anexo2.pdf
- NAM-MEC-001-0_Calculo_mecanico_dique_Anexo3.pdf
- NAM-MEC-001-0_Calculo_mecanico_dique.pdf
- NAM-MEM-003_11-Detalles_tipicos.pdf
- NAM-MEM-003_12_Desarrrollo_de_laminas.pdf
- NAM-PID-039_Dique_tanques_30AIB-Rev0.pdf
- NAM-PIP-012-MAQUETA_3D_INCLUYENDO_ELEMENTOS_CIVILES,_TUBERÍA,_TANQUE_Y_DIQUE_
- NAM-PRG-002-Filosofia_de_Operacion-Rev_0.pdf

./Corresp/2017-06-26-01-initial-info/Nueva carpeta:

- Ensamble_General.stp
- NAM-MEM-003_11-Detalles_tipicos.pdf

Dike nozzle displacements, Release 2.0

- NAM-MEM-003_12_Desarrrollo_de_laminas.pdf

• NAM-PIP-012-MAQUETA_3D_INCLUYENDO_ELEMENTOS_CIVILES,_TUBERÍA,_TANQUE_Y_DIQUE_

This document:

• directory: ./report

• report source: Dike-displacements-report.rst

• ./report/_build/latex: Dike_nozzle_displacements.pdf and Dike_nozzle_displacements.tex

• image on the front page, deformed shape, Case 6, colors for DX, scale factor 40, color scale

−12.9 .. − 3 [mm]: /report/images/cover-border.png reported results:

• main results, directory: ./FEM/v00_10_different_ref_temp

• generate geometry and mesh: dike_v00_10_geom.py

• database file: Study1_v00_10.hdf

• code_aster command ThermoMech_v00_10.comm

• extract deformations table: processResuFile.py

• graphic postProcessing script: postProccessParaview.py

• relative displacements to dike bottomL ./FEM/v00_15_as_v00_10_with_rel_displacements appendix results:

• ./FEM/v00_11_change_soil_size

• ./FEM/v00_12_different_soil_prop

• ./FEM/v00_13_different_mesh

• ./FEM/v01_00_include_inner_wal Chapter 6. APPENDIX A – Files

7. APPENDIX B – DRAWINGS

This appendix presents images of the drawings used for this report for indication purposes only.

Figure 7.1 NAM-MEM-003_11, rev 0, AB-2105-003, Ingenieria de detaille diques tanques 30A/30B amoniaco detailles generales.

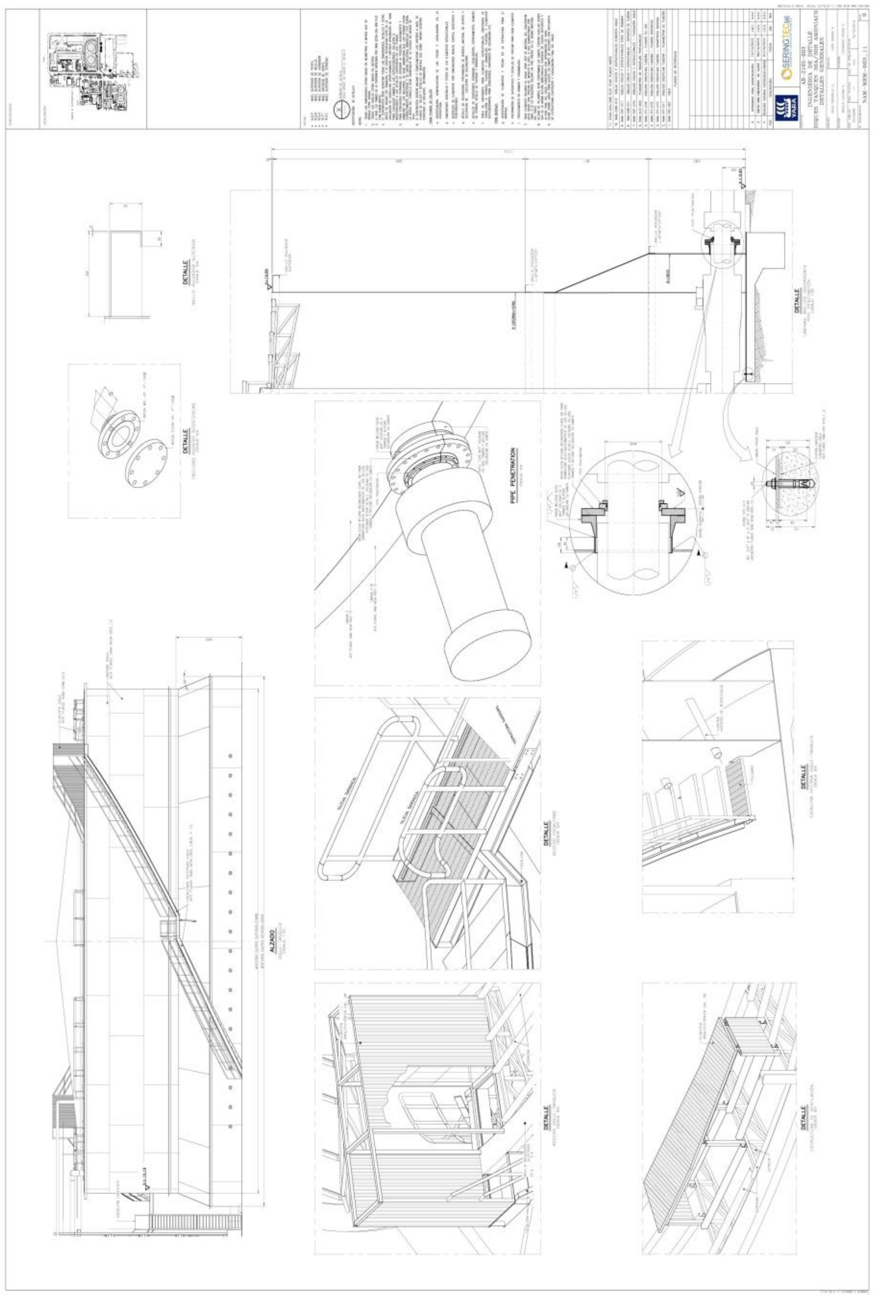

Figure 7.2: NAM-MEM-003_12, rev 0, Ingeneria de detaille diques tanques 30A / 30B amoniaco dessarollo de laminas dique TK30A/30B.

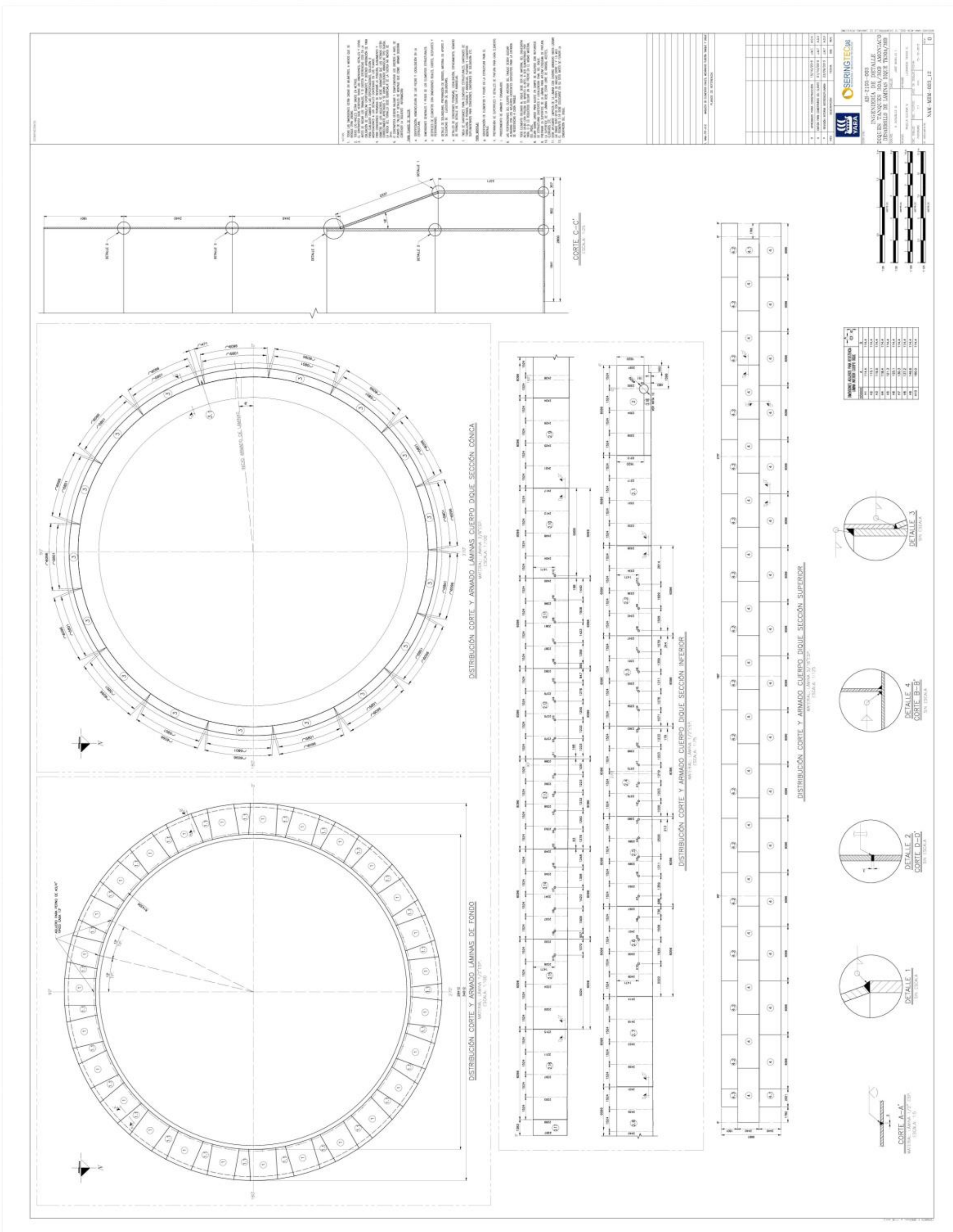

8. APPENDIX C – IMPACT OF SOILSIZE AND PROPERTIES ON RESULTS

8.1. IMPACT OF SOIL SIZE

Only a part of the soil is modeled, and a quasi-static temperature distribution is calculated. Hence, the shape and size of the soil determines this distribution to a large extend.

This paragraph studies the effect of the size and shape of the modeled soil on the nozzle deformations.

Here, the soil is modeled with the sizes: Ro,soil = 1.5 · Ro,dike,bottom and Hsoil = 5 [m].

The calculated radial deformations are almost equal to the main reported calculation, except case 6, where a difference of 3% which is negligible compared to the change in soil size. Differences in DY deformations can be observed for all Cases, which is due to less soil compression or contraction, simply because there is less soil to contract.

It is concluded here, that the assumptions of the soil size in the main FEM model are accurate enough.

Case	DX [mm]	DY [mm]	ANG [deg]
Case 1, Gravity	0.011	-0.005	-0.001
Case 2, weight of the roof	0.001	-0.000	-0.000
Case 3, hydrostatic pressure	4.294	-0.053	-0.358
Case 4, minimum outside temperature	-1.557	-0.809	0.135
Case 5, maximum outside temperature	1.557	0.809	-0.135
Case 6, $-33[°C]$ of failed ammonia tank	-10.370	-3.954	0.679

8.2. IMPACT OF SOIL PROPERTIES

The properties of the soil are assumed while literature gives large value ranges for soil properties. This paragraph studies the impact of the soil properties on the overall results. The used properties are given in the table below. All properties are approximately 20% lower than the original value, except the density, which is about 20% higher.

Table 8.1: Soil material properties

Material	Density ρ $[kg/m]$	Elasticity $[Pa]$	Poisson ratio ν $[-]$	Thermal expansion coefficient α $[m/mK]$	Thermal conductivity coefficient λ $[W/mK]$
Soil in main calculation	1300	$24 \cdot 10^6$	0.45	$12 \cdot 10^{-6}$	$2 \cdot 10^{-6}$
Soil in this appendix	1560	$20 \cdot 10^6$	0.40	$10 \cdot 10^{-6}$	$1.6 \cdot 10^{-6}$

The calculated deformations for these properties are listed below. The differences to the main FEM calculation are less than 2% in radial direction, which is a factor 10 lower than the applied changes. Hence, the results are not very sensitive to the soil properties.

Case	DX [mm]	DY [mm]	ANG [deg]
Case 1, Gravity	0.011	-0.021	-0.001
Case 2, weight of the roof	0.001	-0.000	-0.000
Case 3, hydrostatic pressure	4.293	-0.059	-0.359
Case 4, minimum outside temperature	-1.562	-1.220	0.133
Case 5, maximum outside temperature	1.562	1.220	-0.133
Case 6, $-33[°C]$ of failed ammonia tank	-10.546	-5.243	0.624

9. APPENDIX D – IMPACT OF MESH SIZE ON RESULTS

When, the mesh size is increased with a factor 2, the deformations increase with a factor 0.4%, hence the Mesh size is sufficiently small.

Case	DX [mm]	DY [mm]	ANG [deg]
Case 1, Gravity	0.011	-0.010	-0.001
Case 2, weight of the roof	0.001	-0.000	-0.000
Case 3, hydro-static pressure	4.302	-0.057	-0.358
Case 4, minimum outside temperature	-1.560	-1.589	0.135
Case 5, maximum outside temperature	1.560	1.589	-0.135
Case 6, $-33[°C]$ of failed ammonia tank	-10.708	-6.521	0.577

10. APPENDIX E – IMPACT INCLUDING INNER WALL ON RESULTS

The inner wall is not present in the full circumference of the dike. Therefore, the FEM model in this report does not include the inner wall. An exception is this appendix, where the impact of the inner wall inclusion is evaluated on the results.

The geometry of the inner-wall is added to the dike as shown below and meshed with the same mesh properties as the rest of the model.

The same material properties as for the rest of the dike is applied to the dike, except for the Elasticity module E, according to the equations below. the E-module for the inner wall top is reduced to account for the gap. In an axi-symmetric model, the stiffness of this hole is smeared out over the full circumference. Hence, the results are not exact, but at least slightly better than no E-module correction.

$$E_{innerwall,top} = \frac{angle_{innerwall}}{360°} \cdot E_{steel} = \frac{341.7}{360} 210 \cdot 10^9 = 199 \cdot 10^9 \; [Pa]$$

In the bottom section of the inner wall, additional slots are present and the E-module here is reduced further, using equation:

$$E_{innerwall,bot} = \frac{angle_{material}}{angle_{material} + angle_{slot}} \cdot E_{innerwall,top} = \frac{4.22}{4.22 + 1.09} \cdot 199 \cdot 10^9 = 158 \cdot 10^9 \; [Pa]$$

This $E_{innerwall,bot}$ is applied over a height of $H_{innerwall,bot} = 177.5\ [mm]$.

In case 3, the hydro-static pressure is applied on both the inner and outer wall, as it is assumed there will be a hole where the air above the ammonia can escape.

In case 6, the temperature is also applied on both inner and outer wall, because at least the conduction of the steel will make sure everything will be at or close to the ammonia boiling temperature.

Case	DX [mm]	DY [mm]	ANG [deg]
Case 1, Gravity	0.004	-0.009	-0.000
Case 2, weight of the roof	0.000	-0.000	-0.000
Case 3, hydro-static pressure	4.270	-0.052	-0.357
Case 4, minimum outside temperature	-1.555	-1.590	0.135
Case 5, maximum outside temperature	1.555	1.590	-0.135
Case 6, $-33 [°C]$ of failed ammonia tank	-10.678	-6.530	0.578

The results are listed in the above table. For case 3 and 6 differences in DX deformations in the order of $\Delta DX \approx 0.03\ [mm]$, which is approximately 0.3%. A deformation plot for case 6 is shown below.

Figure 10.1. FEM model geometry with inner wall included.

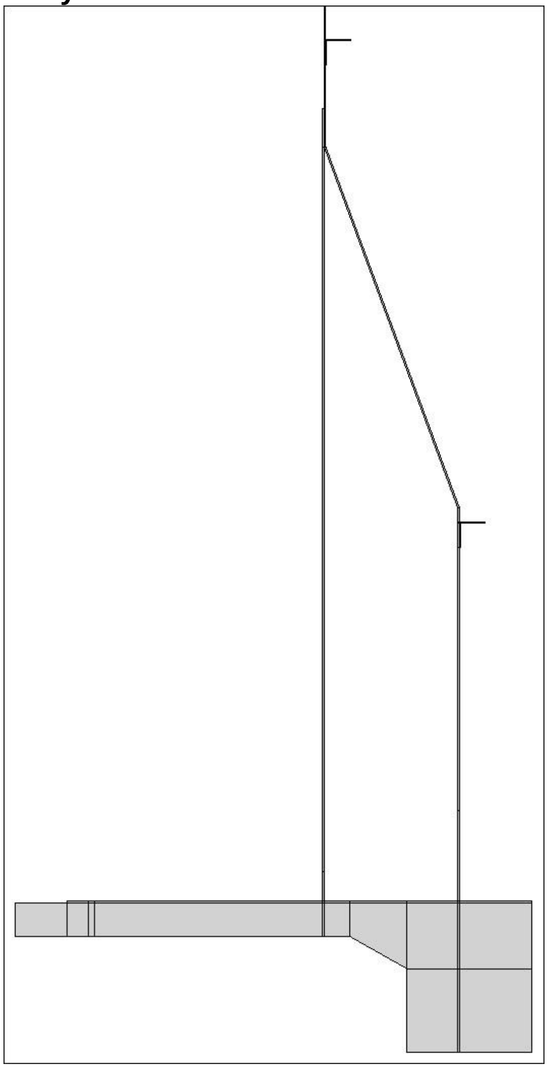

The results are listed in the above table. For case 3 and 6 differences in DX deformations in the order of $\Delta DX \approx 0.03\ [mm]$, which is approximately 0.3%. A deformation plot for case 6 is shown below.

Figure 10.2. Case 6: Thermal deformation due to failed inner tank, deformation in radial direction, zoom in on POI including inner wall.

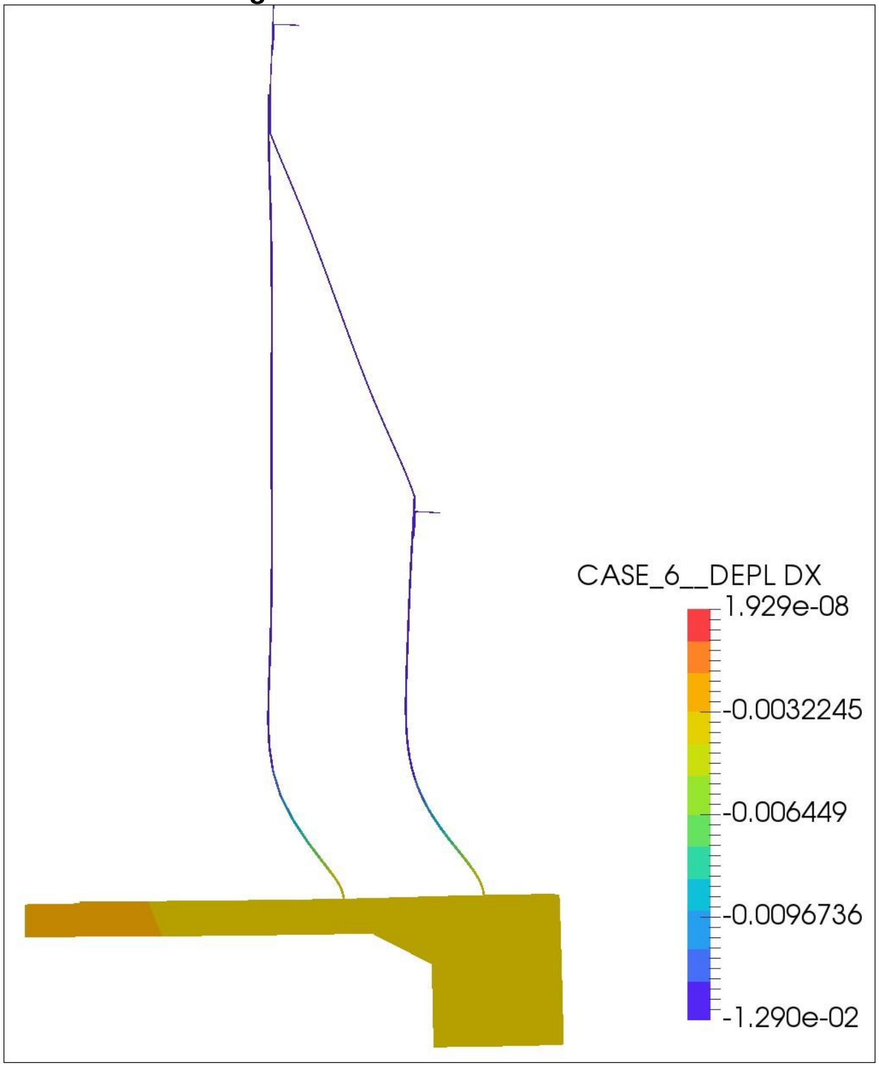

In can be concluded that the inner wall is a negligible influence on the nozzle displacements. The low impact of the inner wall on the displacements of the nozzle by low out-of-plane bending stiffness of the inner-wall, that must be transferred through foundation and conical plate to the nozzle.

11. APPENDIX F – FEM INPUT PARAMETERS

The input parameters in the FEM model for latest calculation, documented in APPENDIX E – Impact including inner wall in model on results.

```
###
### Parameters
###

# general
inch = 0.0254
zero = 1e-6
inf  = 1e6

# site
N     = 8.650

# Foundation
found_Ro = 17.005
found_W  =  3.110
found_H  =  0.900
found_t1 =  0.200
found_w1 =  2.015
found_t2 =  0.195 + found_t1
found_w2 =  2.360
found_Ri = found_Ro - found_W
found_R1 = found_Ri + found_w1
found_R2 = found_Ri + found_w2
found_BR = 14.356
found_Bd = 3. / 4 * inch
found_B1 = found_BR - found_Bd   # Connection is larger than hole, here␣
↪assumed factor 2
found_B2 = found_BR + found_Bd

# Soil
soil_Ro  = 2 * found_Ro
soil_H   = 10.0

# Dike
dike_H = 19.80 - N
```

```
# Dike bottom plate
dikeBot_Ro = 16.572
dikeBot_Ri = 14.206
dikeBot_t  = 1. / 2 * inch
dikeBot_Ho = 2.36521
dikeBot_Hi = 2.371

# Dike outer plate
dikeOut_Ro = 16.572
dikeOut_t  = 1. / 2 * inch

# Dike diagonal plate
dikeDia_t = 3. / 8 * inch
dikeDia_H1 = 4.54135
dikeDia_H2 = 0.00573139

# Dike upper plate
dikeUpp_Ro = 15.765
dikeUpp_t  = 5. / 16 * inch
dikeUpp_H1   = 4.77439

# Dike inner plate
dikeInn_Ro = dikeUpp_Ro - dikeUpp_t
dikeInn_t =  1. / 2 * inch
dikeInn_H1 = 0.177505

# two bottom ring stiffeners, shape L, dimensions from drawing
dikeRingBot_L   = 6.0 * inch
dikeRingBot_t   = 0.25 * inch
dikeRingBot_H1 = 2.283
dikeRingBot_H2 = 2.911 + dikeRingBot_H1

# one upper ring stiffener, shape U, dimensions from Detail drawing
dikeRingTop_w1 = 0.356
dikeRingTop_H   = 0.152
dikeRingTop_w2 = 0.064
dikeRingTop_H3 = 5.955 + dikeRingBot_H2
dikeRingTop_t   = 0.006

# Ammonia
ammonia_H = 8.433

# POI
poi_H = 0.546

# switches
hasInnerWall = True
addGeom = False

################### Mesh

MeshSizeLarge = 15
MeshSizeWall = 4
```

12. APPENDIX F – AXISYMMETRIC

For Axisymmetric elements Salome Meca See r3.06.04 CODEL ASTER document.
For axisymmetric FEA Theory see
http://abaqusdoc.ucalgary.ca/books/stm/default.htm?startat=ch03s02ath66.html